

Mixed Coherent and Non-Coherent Transmission for Multi-CPU Cell-Free Systems

Roberto P. Antonoli^{*,*}, Iran M. Braga Jr.^{*}, Gábor Fodor^{†‡}, Yuri C. B. Silva^{*}, Walter C. Freitas Jr.^{*}

Wireless Telecom Research Group (GTEL)^{*}, Federal University of Ceará, Fortaleza, Brazil.

Instituto Atlântico^{*}, Fortaleza, Brazil. Ericsson Research[†] and Royal Institute of Technology[‡], Stockholm, Sweden.
{antonoli, iran, yuri, walter}@gtel.ufc.br, roberto_antonoli@atlantico.com.br, gabor.fodor@ericsson.com, gaborf@kth.se

Abstract—Existing works on cell-free systems consider either coherent or non-coherent downlink data transmission and a network deployment with a single central processing unit (CPU). While it is known that coherent transmission outperforms non-coherent transmission when assuming unlimited fronthaul links, the former requires a perfect timing synchronization, which is practically not viable over a large network. Furthermore, relying on a single CPU for geographically large cell-free networks is not scalable. Thus, to realize the expected gains of cell-free systems in practice, alternative transmission strategies for realistic multi-CPU cell-free systems are required. Therefore, this paper proposes a novel downlink data transmission scheme that combines and generalizes the existing coherent and non-coherent transmissions. The proposed transmission scheme, named mixed transmission, works based on the realistic assumption that only the access points (APs) controlled by a same CPU are synchronized, and thus transmit in a coherent fashion, while APs from different CPUs require no synchronism and transmit in a non-coherent manner. We also propose extensions of existing clustering algorithms for multi-CPU cell-free systems with mixed transmission. Simulation results show that the combination of the proposed clustering algorithms with mixed transmission have the potential to perform close to the ideal coherent transmission.

Index Terms—Cell-free, clustering algorithms, mixed transmission.

I. INTRODUCTION

The cell-free multiple input multiple output (MIMO) architecture was conceived with the goal of eliminating cell boundaries and providing uniformly great service to every user in the system. In the canonical form of the cell-free architecture, the network deployment follows a star topology, in which many distributed access points (APs) have independent fronthaul connections to a single central processing unit (CPU). However, it is unlikely that practical deployments of cell-free systems in geographically large networks will rely on a single CPU, since the idea that the entire network would act as an infinitely large single cell, comprised by a single CPU and all the APs, is not scalable. Moreover, the common assumption that the data from all APs would be processed in a coherent manner is not scalable [1] either. In realistic large cell-free scenarios, the most likely deployment will comprise multiple CPUs, and each CPU controls a disjoint set of APs [1], [2].

Both in the canonical and multi-CPU cell-free cases, achieving a sufficiently accurate relative timing and phase synchronization, such that all APs can jointly exploit coherent signal processing, is not a simple task. Indeed, the communication

theory underlying coherent transmissions for cell-free systems assumes that a perfect timing synchronization exists, which is physically impossible over a large network, even if the clocks from the APs are synchronized [2]. Besides that, joint coherent transmission requires that the data to be transmitted to a certain user be simultaneously available at multiple APs [3]–[5]. Such strict requirements might be difficult to achieve even in centralized solutions [3], [6], and therefore it deserves further investigation in the cell-free context [2], [7].

The majority of works on cell-free MIMO have considered coherent downlink data transmission in scenarios with unlimited fronthaul, such as in [1], [8]–[12]. Assuming non-coherent downlink data transmission, a resource allocation for cell-free MIMO is proposed in [13]. Some papers compared coherent and non-coherent downlink data transmissions in cell-free systems under the assumption of unlimited fronthauls [14], [15], and concluded that coherent transmission always outperforms non-coherent transmission in such scenarios. In [16], the authors compared coherent and non-coherent transmission considering the realistic assumption of limited fronthauls, and showed that non-coherent transmission outperforms coherent transmission in scenarios with low fronthaul capacities.

While the studies considering coherent downlink transmission in cell-free MIMO systems proposed solutions that are transparent to the underlying cell-free topology, they assumed perfect network-wide synchronization, which is physically impossible [2]. Therefore, such an idealized coherent transmission can be only seen as an upper bound for the performance that can be achieved in practice by cell-free systems. Thus, alternative transmission strategies that do not rely on network-wide synchronization are desired [17].

In this work, we consider a practically feasible scenario with multiple CPUs controlling disjoint clusters of APs, in which the multiple CPUs are not perfectly synchronized, such that the APs from different CPUs are not capable of serving a certain user equipment (UE) using coherent transmission. We assume accurate synchronization and simultaneous data availability only within the APs from each CPU. In this context, we go beyond the existing works and propose a novel transmission scheme that combines and generalizes the existing coherent and non-coherent transmissions. When considering multi-CPU cell-free systems and the proposed mixed transmission, some existing algorithms need to be redesigned. Along this line, we extend three existing clustering algorithms. Computational

simulations considering multi-CPU cell-free systems with correlated fading, multi-antenna APs and pilot contamination analyze the performance of the proposed clustering solutions and indicate that the mixed transmission performs close to the coherent transmission.

Notation: Throughout the paper, matrices and vectors are presented by boldface upper and lower case letters, respectively. $(\cdot)^T$ and $(\cdot)^H$ denote the transpose and conjugate transpose operations, respectively. $\{x_i\}_{\forall i}$ denotes the set of elements x_i for the values of i denoted by the subscript expression. \mathbf{I} is the identity matrix. The cardinality of a discrete set \mathcal{X} is denoted by $|\mathcal{X}|$. Expected value of a random variable is denoted by $\mathbb{E}[\cdot]$.

II. SYSTEM MODEL

We consider the downlink of a cell-free system comprised of M APs, each equipped with N antennas, and K single-antenna UEs. Let \mathcal{M} and \mathcal{K} be the sets of APs and UEs, respectively, where $|\mathcal{M}| = M$ and $|\mathcal{K}| = K$. The APs are connected via fronthaul links to CPUs, where the set of CPUs is denoted as \mathcal{Q} , with $|\mathcal{Q}| = Q$. The subset of APs connected to CPU q is denoted by $\mathcal{V}_q \subset \mathcal{M}$. We consider a user-centric cell-free system in which each UE k is served only by a subset of nearby APs, denoted herein as $\mathcal{A}_k \subset \mathcal{M}$, where $|\mathcal{A}_k| = A_k$. The subset of UEs served by AP m is denoted by $\mathcal{U}_m \subset \mathcal{K}$.

In the existing literature, it is commonly assumed that the set of APs \mathcal{A}_k serves each UE k using coherent transmission, in which the same data symbols are transmitted by all APs in \mathcal{A}_k to UE k [9]. Alternatively, some studies considered that the APs in \mathcal{A}_k serve UE k by means of non-coherent transmission, where the APs in \mathcal{A}_k transmit different data symbols to UE k [14], [15]. When non-coherent transmission is considered, each single-antenna UE k decodes the data symbols from different APs using successive interference cancellation (SIC).

Herein, we go beyond the existing models from the literature and develop a mixed coherent-and-non-coherent transmission, denoted hereafter as mixed transmission, in which the set \mathcal{A}_k is partitioned into sets of APs \mathcal{A}_k^c . It is assumed that $\mathcal{A}_k^c \cap \mathcal{A}_k^{c'} = \emptyset$, $c \neq c'$ and $\bigcup_{\forall c} \mathcal{A}_k^c = \mathcal{A}_k$. The set of coherent groups serving UE k is denoted as \mathcal{C}_k , where $|\mathcal{C}_k| = C_k \leq A_k$. All APs within set \mathcal{A}_k^c are synchronized and serve UE k in a coherent fashion, thus sending the same data symbols to UE k . Each set \mathcal{A}_k^c is herein referred to as a coherent group. While the APs within \mathcal{A}_k^c send the same data symbols to UE k , the symbols transmitted by the APs in $\mathcal{A}_k^{c'}$ are different from the ones transmitted by the APs in \mathcal{A}_k^c . In this way, the APs from set \mathcal{A}_k^c do not need to be synchronized with the APs from set $\mathcal{A}_k^{c'}$. Therefore, transmissions from different coherent groups occur in a non-coherent fashion, such that the data symbols transmitted by different coherent groups need to be decoded by the UEs using SIC.

The APs and users operate a time division duplex (TDD) protocol, consisting of an uplink pilot phase used for channel estimation, followed by a downlink data transmission phase.

The channels estimated in the pilot phase are used by the APs for precoding in the downlink data transmission phase, which is a valid assumption that relies on the channel reciprocity provided by TDD [4], [7].

We assume that the channel vector $\mathbf{h}_{m,k} \in \mathbb{C}^{N \times 1}$ between user k and AP m follows a standard block fading model. Therefore, $\mathbf{h}_{m,k}$ is constant in time-frequency blocks of τ_c symbols, where τ_c is the length of the coherence block. Independent channel realizations are drawn in each coherent block following a correlated Rayleigh distribution [9]:

$$\mathbf{h}_{m,k} \sim \mathcal{N}_{\mathbb{C}}(\mathbf{0}, \mathbf{R}_{m,k}), \quad (1)$$

where $\mathbf{R}_{m,k} \in \mathbb{C}^{N \times N}$ is the spatial correlation matrix of the channel between user k and AP m , and $\beta_{m,k} \triangleq \frac{\text{tr}(\mathbf{R}_{m,k})}{N}$ is the large scale fading (LSF) coefficient, which includes pathloss and shadowing.

A. Pilot Phase and Channel Estimation

We assume that τ_p mutually orthogonal pilot sequences $\varphi_1, \dots, \varphi_{\tau_p} \in \mathbb{C}^{\tau_p}$ are used for channel estimation. Each user is assigned a pilot sequence during the initial access procedure, where such an assignment is done in a deterministic but arbitrary way and $\|\varphi_t\|^2 = \tau_p$. In practical scenarios, it commonly happens that there are more users than available orthogonal pilot sequences in the system, i.e., $K > \tau_p$. Thus, multiple users will share the same pilot sequence, giving rise to pilot contamination. This situation is modeled herein using the set $\mathcal{P}_k \subset \mathcal{K}$, which represents the subset of users sharing the same pilot assigned to user k , including itself. Also, let $t_k \in \{1, \dots, \tau_p\}$ denote the index of the pilot sequence assigned to user k .

The received pilot signal matrix $\mathbf{Y}_m^p \in \mathbb{C}^{N \times \tau_p}$ at the AP m is given by

$$\mathbf{Y}_m^p = \sum_{k=1}^K \sqrt{p_k^p} \mathbf{h}_{m,k} \varphi_{t_k}^H + \mathbf{N}_m^p, \quad (2)$$

where $p_k^p \geq 0$ is the pilot power of user k and $\mathbf{N}_m^p \in \mathbb{C}^{N \times \tau_p}$ is the received noise at AP m with independent $\mathcal{N}_{\mathbb{C}}(0, \sigma^2)$ entries, where σ^2 is the noise power.

The channel estimation is conducted at AP m by projecting \mathbf{Y}_m^p onto the associated normalized pilot signal $\varphi_{t_k}/\sqrt{\tau_p}$, which results in $\tilde{\mathbf{y}}_{m,t_k} = \frac{1}{\sqrt{\tau_p}} \mathbf{Y}_m^p \varphi_{t_k} \in \mathbb{C}^N$. Then, the minimum mean squared error (MMSE) estimate of $\mathbf{h}_{m,k}$ is [9]

$$\hat{\mathbf{h}}_{m,k} = \sqrt{p_k^p \tau_p} \mathbf{R}_{m,k} \Psi_{m,t_k}^{-1} \tilde{\mathbf{y}}_{m,t_k}, \quad (3)$$

where

$$\Psi_{m,t_k} = \mathbb{E} \{ \tilde{\mathbf{y}}_{m,t_k} \tilde{\mathbf{y}}_{m,t_k}^H \} = \sum_{i \in \mathcal{P}_k} \tau_p p_i^p \mathbf{R}_{m,i} + \sigma^2 \mathbf{I}_N \quad (4)$$

is the correlation matrix of $\tilde{\mathbf{y}}_{m,t_k}$. The estimated $\hat{\mathbf{h}}_{m,k}$ and the channel estimation error $\tilde{\mathbf{h}}_{m,k} = \mathbf{h}_{m,k} - \hat{\mathbf{h}}_{m,k}$ are independent vectors distributed as $\hat{\mathbf{h}}_{m,k} \sim \mathcal{N}_{\mathbb{C}}(\mathbf{0}, p_k^p \tau_p \mathbf{R}_{m,k} \Psi_{m,t_k}^{-1} \mathbf{R}_{m,k})$ and $\tilde{\mathbf{h}}_{m,k} \sim \mathcal{N}_{\mathbb{C}}(\mathbf{0}, \mathbf{C}_{m,k})$, in which $\mathbf{C}_{m,k} = \mathbb{E} \{ \tilde{\mathbf{h}}_{m,k} \tilde{\mathbf{h}}_{m,k}^H \} = \mathbf{R}_{m,k} - p_k^p \tau_p \mathbf{R}_{m,k} \Psi_{m,t_k}^{-1} \mathbf{R}_{m,k}$.

B. Mixed Downlink Data Transmission and Closed-Form SE

Since this work focuses on the downlink transmission, we consider that $\tau_d = \tau_c - \tau_p$ symbols are reserved for downlink transmission. The channels locally estimated at the APs based on the MMSE estimator given in (3) are treated as the true channels, and are used for maximum ratio (MR) beamforming during the downlink transmission, which is given by [7], [9]

$$\mathbf{w}_{m,k}^{\text{MR}} = \sqrt{\rho_{m,k}} \frac{\hat{\mathbf{h}}_{m,k}}{\sqrt{\mathbb{E}\left\{\|\hat{\mathbf{h}}_{m,k}\|^2\right\}}}, \quad (5)$$

in which $\hat{\mathbf{h}}_{m,k}$ is the MMSE channel estimate from (3) and $\rho_{m,k} \geq 0$ is the data power from AP m to user k , with $\sum_{k \in \mathcal{U}_m} \rho_{m,k} \leq \mathbf{P}_m^{\max}$, where \mathbf{P}_m^{\max} is the power budget of AP m .

In the mixed downlink transmission, each AP within the coherent group \mathcal{A}_k^c coherently transmits the same data symbol to the intended user k , while the APs from different coherent groups $\mathcal{A}_k^{c'}$, $c \neq c'$, transmit different symbols in a non-coherent fashion. The signal received by user k is given by:

$$y_k = \sum_{c \in \mathcal{C}_k} \sum_{m \in \mathcal{A}_k^c} \mathbf{h}_{m,k}^H \mathbf{w}_{m,k} s_k^c + \sum_{\substack{i \neq k \\ i \in \mathcal{K}}} \sum_{c \in \mathcal{C}_i} \sum_{m \in \mathcal{A}_i^c} \mathbf{h}_{m,k}^H \mathbf{w}_{m,i} s_i^c + z_k, \quad (6)$$

where $s_k^c \in \mathbb{C}$, with $\mathbb{E}\{|s_k^c|^2\} = 1$, is the transmitted data symbol transmitted by the APs from \mathcal{A}_k^c to UE k , $z_k \sim \mathcal{N}_{\mathbb{C}}(0, \sigma_k^2)$ is the additive white Gaussian noise at UE k , and $\mathbf{w}_{m,k}$ is the downlink beamforming vector from AP m to UE k .

To obtain a closed-form expression of the downlink spectral efficiency (SE) lower bound, we assume that the APs use MR precoding from (5) with the MMSE channel estimation from (3), as shown next.

Lemma 1. *Based on the received signal model in (6), using MR precoder in (5) and the MMSE channel estimation in (3), a closed-form SE achieved by the coherent group c when transmitting to user k is*

$$r_k^c = \frac{\tau_d}{\tau_c} \log_2(1 + \gamma_k^c), \quad (7)$$

where

$$\gamma_k^c = \frac{\mathbf{D}_k^c}{\mathbf{E}_k + \mathbf{F}_k - \sum_{b=1}^c \mathbf{D}_k^b + \sigma_k^2}, \quad (8)$$

$$\mathbf{D}_k^c = \left| \sum_{m \in \mathcal{A}_k^c} \sqrt{\rho_{m,k} p_k^p \tau_p \text{tr}(\mathbf{R}_{m,k} \Psi_{m,t_k}^{-1} \mathbf{R}_{m,k})} \right|^2, \quad (9)$$

$$\mathbf{E}_k = \sum_{i \in \mathcal{K}} \sum_{b \in \mathcal{C}_i} \sum_{m \in \mathcal{A}_i^b} \rho_{m,i} \frac{\text{tr}(\mathbf{R}_{m,k} \mathbf{G}_{i,i})}{\text{tr}(\mathbf{G}_{i,i})}, \quad (10)$$

$$\mathbf{F}_k = \sum_{i \in \mathcal{K}} \sum_{b \in \mathcal{C}_i} \left| \sum_{m \in \mathcal{A}_i^b} \sqrt{\rho_{m,i} p_k^p \tau_p \frac{\text{tr}(\mathbf{G}_{i,k})}{\sqrt{\text{tr}(\mathbf{G}_{i,i})}}} \right|^2 \left(\frac{\boldsymbol{\varphi}_{t_k}^H \boldsymbol{\varphi}_{t_i}}{\tau_p} \right), \quad (11)$$

$$\mathbf{G}_{i,k} = \mathbf{R}_{m,i} \Psi_{m,t_k}^{-1} \mathbf{R}_{m,k}. \quad (12)$$

Moreover, the closed-form total SE achieved by user k for the mixed transmission strategy is given by $r_k = \sum_{c \in \mathcal{C}_k} r_k^c$.

Proof. This proof can be conducted following [7, Section 6.2]. \square

The rate expression derived in Lemma 1 for the proposed mixed transmission is a generalization of the rate expressions of the existing coherent and non-coherent transmissions since the proposed mixed transmission particularizes to those two cases. Specifically, observing (7), one can see that the mixed transmission reduces to the coherent case when there is only one large coherent group serving each user k in a coherent fashion, i.e., $|\mathcal{C}_k| = C_k = 1$ and $|\mathcal{A}_k^1| = A_k$. This scenario where all APs from the unique coherent group $\mathcal{A}_k^1, \forall k \in \mathcal{K}$ serve each user $k \in \mathcal{K}$ in a coherent fashion would only be possible in an ideal situation, where all CPUs are perfectly synchronized. Note that the mixed transmission rate expression in (7) reduces to the non-coherent transmission if we consider that all coherent groups serving each user k have only one AP, i.e., $|\mathcal{C}_k| = C_k = A_k$ and $|\mathcal{A}_k^c| = 1, \forall c \in \mathcal{C}_k$.

III. CLUSTERING ALGORITHMS

This section proposes extensions of existing clustering algorithms – which have been designed for single CPU systems – to multi-CPU cell-free systems using mixed transmissions. We remark that the clustering algorithms proposed herein form clusters by adding one UE at a time as proposed in [7]. However, our proposed schemes control the number of coherent groups using mixed transmissions by setting a control parameter n_{CPU} , as detailed next.

A. LSF Larger Than Threshold

The first proposed algorithm selects the APs from the n_{CPU} best CPUs with LSF larger than a predefined threshold. The CPUs are ordered based on the following rule: (1) for each k , we select the AP from each CPU q with the largest LSF coefficient $\beta_{m,k}, m \in \mathcal{V}_q$; (2) then, the CPUs are ordered (in descending order) based on the LSF values of their best AP with respect to user k ; (3) after ordering the CPUs, we select the n_{CPU} best CPUs and consider only the APs from those n_{CPU} best CPUs for the cluster formation, i.e., only $m \in \bigcup_{q=1}^{n_{\text{CPU}}} \mathcal{V}_q$. Finally, after ordering the CPUs, the APs meeting $\beta_{m,k} \geq \Delta$ are selected to serve user k , where Δ is a threshold of minimum required large scale fading quality. This clustering algorithm is referred to as *LSF algorithm* hereafter. We highlight that setting n_{CPU} to the number of CPUs in the system corresponds to reducing the proposed solution to the legacy solution from [18], in which each user could be served by all APs in the system.

B. Fixed Number of APs

The second proposed algorithm selects a fixed number of APs n_{AP} from the n_{CPU} best CPUs. First, the CPUs are ordered based on the same rule of the previous solution and the values of $\beta_{m,k} \in \bigcup_{q=1}^{n_{\text{CPU}}} \mathcal{V}_q$ are sorted in descending order.

After ordering the CPUs, we select the n_{CPU} best CPUs and consider only the APs from those n_{CPU} best CPUs for the cluster formation, i.e., only $m \in \bigcup_{q=1}^{n_{\text{CPU}}} \mathcal{V}_q$. Then, the n_{AP} APs with largest LSF coefficients are selected to compose the cluster serving each user k . This clustering algorithm is referred to as *Fixed algorithm* hereafter. This proposed solution reduces to the solution from [19] when setting n_{CPU} to the number of CPUs in the system.

C. Fraction of Total Received Power

The third proposed clustering algorithm selects the APs from the n_{CPU} best CPUs to make sure that:

$$\frac{\sum_{m \in \mathcal{A}_k} \beta_{m,k}}{\sum_{m \in \bigcup_{q=1}^{n_{\text{CPU}}} \mathcal{V}_q} \beta_{m,k}} \geq \delta, \quad (13)$$

where the CPUs are ordered based on the same rule of the previous solution and the values of $\beta_{m,k} \in \bigcup_{q=1}^{n_{\text{CPU}}} \mathcal{V}_q$ are sorted in descending order. We remark that after ordering the CPUs, we select the n_{CPU} best CPUs and consider only the APs from those n_{CPU} best CPUs for the cluster formation, i.e., only $m \in \bigcup_{q=1}^{n_{\text{CPU}}} \mathcal{V}_q$. Thus, the main idea of this algorithm is to select the APs from the n_{CPU} best CPUs to serve user k that have the strongest channels and that contribute to more than $\delta\%$ of the total power received by user k . This clustering algorithm is referred to as *Power algorithm* hereafter. This proposed multi-CPU clustering solution reduces to the solution in [8] if we set n_{CPU} to the number of CPUs in the system.

IV. NUMERICAL RESULTS AND DISCUSSIONS

A. Parameters and Setup

We consider the downlink of a cell-free system in which APs and users are uniformly distributed in a 1×1 km square, while the CPUs are positioned at fixed locations $([250, 250] \text{ m}, [250, -250] \text{ m}, [-250, -250] \text{ m}$ and $[-250, 250] \text{ m})$. In the considered scenarios, each AP is controlled by the closest CPU. By means of a wrap-around technique, we imitate an infinitely large network. In terms of pilot assignment, we adopt a simple algorithm where each user randomly selects a pilot from a predefined set of orthogonal pilots [8], [20]. The coherence blocks have $\tau_c = 200$ samples and, unless otherwise stated, the number of orthogonal pilots is $\tau_p = 10$. The pilot powers are $p_k^p = 0.2 \text{ W}, \forall k$ and the data powers are $\rho_{m,k} = 0.1 \text{ W}, \forall m, k$, which are not optimized in this paper.

The large-scale coefficients are modeled by path loss and correlated shadowing (in dB): $\beta_{m,k} = \text{PL}_{m,k} + \sigma_{\text{sh}} \varkappa_{m,k}$, where $\sigma_{\text{sh}} \varkappa_{m,k}$ is the shadow fading with standard deviation σ_{sh} and $\varkappa_{m,k} \sim \mathcal{N}(0, 1)$, while $\text{PL}_{m,k}$ represents the path loss given by the three slope model from [8]. For the shadow fading coefficients, we consider the spatially correlated model with two components. The spatial correlation is computed via the Gaussian local scattering model with 15° angular standard deviation [7]. Moreover, the noise power is given

by $\sigma^2 = B\kappa_B T_0 \sigma_F$, where $B = 20 \text{ MHz}$, $\sigma_F = 9 \text{ dB}$, $\kappa_B = 1.381 \times 10^{-23} \text{ Joule per Kelvin}$ and $T_0 = 290 \text{ Kelvin}$.

B. Results and Discussions

In the first simulations, we consider the following setup $\{M, K, N, A_k\} = \{100, 20, 2, 20\}$, where the cluster of APs serving each user k is formed by the A_k APs with the largest values of $\beta_{m,k}$, i.e., we adopt a largest-large-scale-based selection [19]. This is a legacy solution that does not consider the multiple CPUs aspect in the system.

Fig. 1 compares the performance of the mixed, coherent and non-coherent transmissions. The non-coherent transmission obtains the lowest values of total rate, while the coherent transmission achieves the highest values. Meanwhile, the proposed mixed transmission achieves a total rate in between the existing transmission schemes, while being closer to the ideal coherent transmission. The mixed transmission outperforms the non-coherent transmission because of the coherent groups from each CPU that are formed to coherently transmit data to the users, which enhance the desired signal compared to the non-coherent transmission, in which each AP independently transmits data symbols to the users (as if the coherent groups had size of 1). However, even though the formation of the coherent groups enhances the system performance when using the mixed transmission compared to the non-coherent transmission, this performance increase is not enough to reach the performance of the ideal coherent transmission. This occurs because the mixed transmission has some degree of non-coherent transmission from the different coherent groups, which is known to have inferior performance to coherent transmission. Meanwhile, for coherent transmission, all APs must be perfectly synchronized to transmit data to the users.

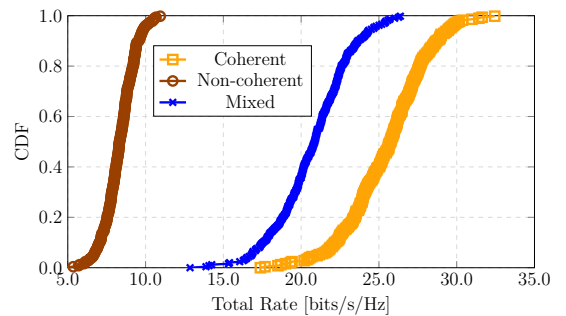


Fig. 1: CDF of total rate comparing the coherent, non-coherent and mixed transmissions.

We now analyze the impact of A_k while still using the largest-large-scale-based selection from [19] as clustering algorithm. The parameters used in this analysis are $\{M, K, N\} = \{100, 20, 2\}$.

Fig. 2 shows the total system rate obtained by coherent, non-coherent and mixed transmissions when the value of A_k is varied. When $A_k = 1$, all three transmission schemes present the same performance because the rate expressions for all three schemes reduce to the same expression. As A_k increases, the rates achieved by the non-coherent transmission steadily decrease. This occurs because of the increasing interference

in the system, which increases faster than the desired signal strength due to the SIC decoding. On the other hand, both mixed and coherent transmissions increase the total rate up to a certain value of A_k , from which point the total rates achieved by these two schemes start decreasing. The reason behind the increase in the total rate achieved by the mixed and coherent transmissions for the smaller values of A_k is because they are able to increase the derived signal strength more than the interference increases. This thinking is valid up to a certain value of A_k , from which the increase in the desired signal strength does not compensate the increase in the interference and pilot contamination, thus decreasing the total rate.

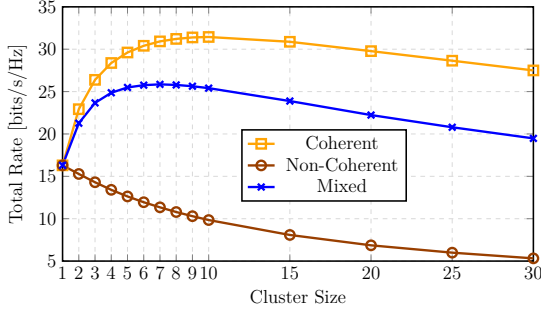


Fig. 2: Total rate comparing coherent, non-coherent and mixed transmissions when varying A_k .

The next figures analyze the performance of the coherent, non-coherent and mixed transmissions when adopting the clustering algorithms proposed in Section III. The parameters used for the clustering algorithms are: $n_{\text{CPU}} = \{1, 2, 4\}$, $\Delta = \{23.5, 64.36, 266.06\}$, $\delta = \{0.85, 0.90, 0.95\}$ and $n_{\text{AP}} = \{5, 10, 15\}$. The system parameters used in this subsection are $\{K, N\} = \{20, 2\}$, while the number of APs is varied.

Fig. 3 shows the total system rate obtained when adopting the Power algorithm. For the mixed transmission, we selected $\delta = 0.95$, which yields the best performance, while varying the parameter n_{CPU} . For the coherent transmission, the best performance occurs when $\delta = 0.95$ and $n_{\text{CPU}} = 2$, which means that the APs from the 2 best CPUs will transmit in a coherent fashion to the users. Meanwhile, for the non-coherent transmission, the best performance occurs when $\delta = 0.85$ and $n_{\text{CPU}} = 1$. It is worth noting that none of the transmission strategies presented their best performances with $n_{\text{CPU}} = 4$, i.e., when using the legacy solution, which shows the importance of multi-CPU-aware clustering solutions. Note that the non-coherent transmission presents its best performance when $\delta = 0.85$, i.e., when the cluster of APs assumes the smallest size considering the analyzed parameters. Meanwhile, both coherent and mixed transmissions present their best performance when creating a larger cluster of APs in a controlled manner by setting $\delta = 0.95$. Moreover, the mixed transmission strategy presented the best performance when the clustering algorithm creates only one large coherent group (i.e., when $n_{\text{CPU}} = 1$), which indicates that the total system rate is not enhanced when adopting multiple non-coherent transmissions from different coherent groups. Also, when $\delta = 0.95$ and $n_{\text{CPU}} = 1$, the

proposed practical mixed transmission strategy achieved a total rate very close to the ideal full coherent transmission.

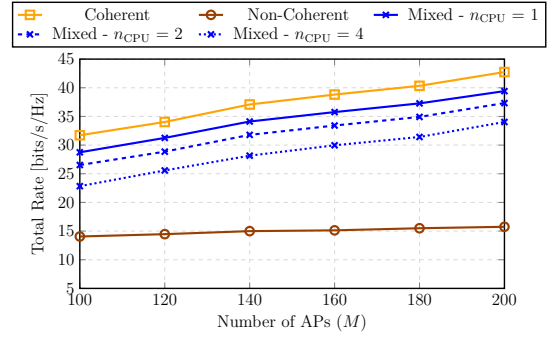


Fig. 3: Impact of the number of different coherent groups on the performance of the mixed transmission with the Power algorithm.

Fig. 4 shows the total rate obtained when adopting the Fixed algorithm. For the mixed transmission, we selected $n_{\text{AP}} = 15$, which yields the best performance, while varying the parameter n_{CPU} . For the coherent transmission, the best performance occurs when $n_{\text{AP}} = 15$ and $n_{\text{CPU}} = 2$. Finally, for the non-coherent transmission, the best performance occurs when $n_{\text{AP}} = 5$ and $n_{\text{CPU}} = 1$. Note again that the analyzed transmission schemes do not reach their best performance when $n_{\text{CPU}} = 4$. As observed previously, the non-coherent transmission achieves its highest performance when using the smallest cluster of APs. Meanwhile, the same conclusions for the mixed transmission discussed for Fig. 3 apply for Fig. 4.

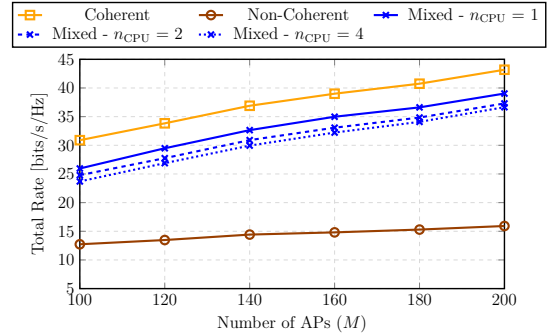


Fig. 4: Impact of the number of different coherent groups on the performance of the mixed transmission with the Fixed algorithm.

Fig. 5 shows the total rate obtained when adopting the LSF algorithm. For the mixed transmission, we selected $\Delta = 23.5$, which yields the best performance, while varying the parameter n_{CPU} . For the coherent transmission, the best performance occurs when $\Delta = 23.5$ and $n_{\text{CPU}} = 4$. Meanwhile, for the non-coherent transmission, the best performance occurs when $\Delta = 266.06$ and $n_{\text{CPU}} = 1$. In particular, for the LSF algorithm, the best performance presented by the coherent transmission was achieved when $n_{\text{CPU}} = 4$, i.e., when using the legacy solution from [18]. The other conclusions from Fig. 3 and Fig. 4 apply to Fig. 5.

Fig. 6 compares the best total rates achieved by the proposed multi-CPU-aware clustering solutions and transmission schemes. The performance obtained by the Power and Fixed

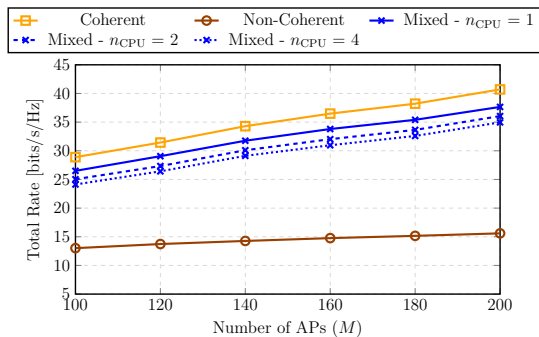


Fig. 5: Impact of the number of different coherent groups on the performance of the mixed transmission with the LSF algorithm.

algorithms are very close for all transmission schemes, with a small advantage to the Power algorithm. The small gain achieved by the Power algorithm comes from its smart AP selection based on a fraction of the received power by each user. Furthermore, the mixed transmission strategy using the Power algorithm presents almost the same performance of the coherent transmission using the LSF algorithm, showing the potential of the mixed transmission scheme and the importance of properly forming the cluster of APs to serve the users.

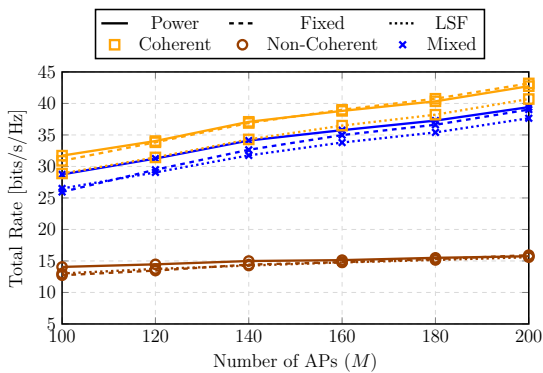


Fig. 6: Comparison of the sum-rate achieved by all clustering algorithms considering their best performances for each transmission scheme.

V. CONCLUSIONS

In this work, we studied multi-CPU cell-free systems with mixed transmission and the impact of the clustering algorithms in these systems. We concluded that legacy clustering algorithms fail to exploit the benefits of the mixed transmission and that the design of multi-CPU-aware clustering algorithms successfully improve the system performance. More specifically, when using the proposed mixed transmission, higher total rates are obtained when forcing the users to be connected to only one CPU and exploiting the coherent transmission potential from that CPU. Also, it was shown that the proposed practical mixed transmission achieves total rates very close to the ideal full coherent transmission, validating its practical viability.

VI. ACKNOWLEDGMENT

This work was supported in part by Ericsson Research, Technical Cooperation Contract UFC.48, in part by CNPq,

in part by FUNCAP, in part by CAPES/PRINT Grant 88887.311965/2018-00, in part by CAPES - Finance Code 001 and in part by the Celtic project 6G for Connected Sky, Project ID: C2021/1-9.

REFERENCES

- [1] G. Interdonato, H. Q. Ngo, P. Frenger, and E. G. Larsson, "Downlink training in cell-free massive MIMO: A blessing in disguise," *IEEE Trans. Wireless Commun.*, vol. 18, no. 11, pp. 5153–5169, Nov. 2019.
- [2] S. Chen, J. Zhang, J. Zhang, E. Björnson, and B. Ai, "A survey on user-centric cell-free massive MIMO systems," *Digital Communications and Networks*, Dec. 2021.
- [3] A. Checko, H. L. Christiansen, Y. Yan, L. Scolari, G. Kardaras, M. S. Berger, and L. Dittmann, "Cloud RAN for mobile networks—a technology overview," *IEEE Commun. Surveys Tuts.*, vol. 17, no. 1, pp. 405–426, Jan. 2015.
- [4] G. Interdonato, E. Björnson, H. Ngo, P. Frenger, and E. Larsson, "Ubiquitous cell-free massive MIMO communications," *EURASIP Journal On Wireless Communications and Networking*, vol. 2019, Aug. 2019.
- [5] Q. D. Vu, L. N. Tran, and M. Juntti, "Noncoherent joint transmission beamforming for dense small cell networks: Global optimality, efficient solution and distributed implementation," *IEEE Trans. Wireless Commun.*, vol. 19, no. 9, pp. 5891–5907, Jun. 2020.
- [6] G. Alexandropoulos, P. Ferrand, J. Gorce, and C. Papadias, "Advanced coordinated beamforming for the downlink of future LTE cellular networks," *IEEE Commun. Mag.*, vol. 54, no. 7, pp. 54–60, Jul. 2016.
- [7] Ö. T. Demir, E. Björnson, and L. Sanguinetti, "Foundations of user-centric cell-free massive MIMO," *Foundations and Trends in Signal Processing*, vol. 14, no. 3-4, pp. 162–472, Jan. 2021.
- [8] H. Q. Ngo, L. Tran, T. Q. Duong, M. Matthaiou, and E. G. Larsson, "On the total energy efficiency of cell-free massive MIMO," *IEEE Trans. Green Commun. Netw.*, vol. 2, no. 1, pp. 25–39, Mar. 2018.
- [9] E. Björnson and L. Sanguinetti, "Scalable cell-free massive MIMO systems," *IEEE Trans. Commun.*, vol. 68, no. 7, pp. 4247–4261, Jul. 2020.
- [10] A. Papazafeiropoulos, H. Q. Ngo, P. Kourtessis, S. Chatzinotas, and J. M. Senior, "Towards optimal energy efficiency in cell-free massive MIMO systems," *IEEE Trans. Green Commun. Netw.*, vol. 5, no. 2, pp. 816–831, Feb. 2021.
- [11] S. Chakraborty, O. Demir, E. Björnson, and P. Giselsson, "Efficient downlink power allocation algorithms for cell-free massive MIMO systems," *IEEE O. J. Commun. Society*, vol. 2, pp. 168–186, Jan. 2021.
- [12] J. Saraiva, R. Antonoli, G. Fodor, W. F. Jr., and Y. C. B., "A distributed game-theoretic solution for power management in the uplink of cell-free systems," in *Proc. IEEE Globecom Workshops*, Dec. 2022.
- [13] H. A. Ammar, R. Adve, S. Shahbazpanahi, G. Boudreau, and K. Srinivas, "Resource allocation and scheduling in non-coherent user-centric cell-free MIMO," in *Proc. IEEE ICC*, Jun. 2021, pp. 1–6.
- [14] Ö. Özdogan, E. Björnson, and J. Zhang, "Performance of cell-free massive MIMO with Rician fading and phase shifts," *IEEE Trans. Wireless Commun.*, vol. 18, no. 11, pp. 5299–5315, Aug. 2019.
- [15] J. Zheng, J. Zhang, E. Björnson, and B. Ai, "Impact of channel aging on cell-free massive MIMO over spatially correlated channels," *IEEE Trans. Wireless Commun.*, pp. 1–1, Apr. 2021.
- [16] R. Antonoli, I. B. Jr., G. Fodor, Y. Silva, A. de Almeida, and W. F. Jr., "On the energy efficiency of cell-free systems with limited fronthauls: Is coherent transmission always the best alternative?" *IEEE Trans. Wireless Commun.*, vol. 21, no. 10, pp. 8729–8743, Oct. 2022.
- [17] S. Varatharajan, M. Grossmann, and G. Del Galdo, "5G new radio physical downlink control channel reliability enhancements for multiple transmission-reception-point communications," *IEEE Access*, vol. 10, pp. 97 394–97 407, 2022.
- [18] E. Björnson, N. Jalden, M. Bengtsson, and B. Ottersten, "Optimality properties, distributed strategies, and measurement-based evaluation of coordinated multicell OFDMA transmission," *IEEE Trans. Signal Process.*, vol. 59, no. 12, pp. 6086–6101, Dec. 2011.
- [19] S. Buzzi and C. D'Andrea, "Cell-free massive MIMO: User-centric approach," *IEEE Wireless Commun. Lett.*, vol. 6, no. 6, pp. 706–709, Dec. 2017.
- [20] T. V. Chien, E. Björnson, and E. G. Larsson, "Joint pilot design and uplink power allocation in multi-cell massive MIMO systems," *IEEE Trans. Wireless Commun.*, vol. 17, no. 3, pp. 2000–2015, Mar. 2018.